Hindawi Publishing Corporation
Journal of Nanomaterials
Volume 2011, Article ID 193510, 10 pages
doi:10.1155/2011/193510

Research Article

Synthesis of Fe_3O_4/Pt Nanoparticles Decorated Carbon Nanotubes and Their Use as Magnetically Recyclable Catalysts

Hongkun He and Chao Gao

MOE Key Laboratory of Macromolecular Synthesis and Functionalization, Department of Polymer Science and Engineering, Zhejiang University, 38 Zheda Road, Hangzhou 310027, China

Correspondence should be addressed to Chao Gao, cgao18@gmail.com

Received 26 July 2010; Accepted 12 October 2010

Academic Editor: Jianyu Huang

We report a facile approach to prepare Fe_3O_4/Pt nanoparticles decorated carbon nanotubes (CNTs). The superparamagnetic Fe_3O_4 nanoparticles with average size of 4 ~ 5 nm were loaded on the surfaces of carboxyl groups functionalized CNTs via a high-temperature solution-phase hydrolysis method from the raw material of $FeCl_3$. The synthesis process of magnetic CNTs is green and readily scalable. The loading amounts of Fe_3O_4 nanopartilces and the magnetizations of the resulting magnetic CNTs show good tunability. The Pt nanopaticles with average size of 2.5 nm were deposited on the magnetic CNTs through a solution-based method. It is demonstrated that the Fe_3O_4/Pt nanoparticles decorated CNTs have high catalytic activity in the reduction reaction of 4-nitrophenol and can be readily recycled by a magnet and reused in the next reactions with high efficiencies for at least fifteen successive cycles. The novel CNTs-supported magnetically recyclable catalysts are promising in heterogeneous catalysis applications.

1. Introduction

The discovery of carbon nanotubes (CNTs) in the early 1990s has vitalized a flurry of research activities over the past decade [1]. Due to their fascinating structural, optoelectronic, physicochemical, and mechanical properties, CNTs serve as an excellent candidate for the model systems of nanoscale science and technology [2–7]. Among the applications of CNTs in various fields, magnetic CNTs (m-CNTs) produced by functionalizing CNTs with magnetic nanomaterials are one of the most useful nanocomposites, which incorporate the features of both magnetism and CNTs, and thus have great potential in biomanipulations [8, 9], alignment [10], contrast agents for magnetic resonance imaging [11], targeted drug delivery [12], and so forth.

Up to date, various kinds of m-CNTs have been synthesized by decorating CNTs with Ni [13], Co [14], CoO [15], Fe [16] nanoparticles, and so forth. Among them, magnetic iron oxide (e.g., maghemite γ-Fe_2O_3 or magnetite Fe_3O_4) nanoparticles have attracted tremendous attentions due to their low toxicity, stability, and biocompatibility in the physiological environment [17–19].

In this regard, numerous reports related to functionalizing CNTs with iron oxide nanoparticles have progressively sprung up, which can be broadly categorized into three methodologies.

(1) The first strategy can be termed as "simultaneous" methodology, in which the nanoparticles and CNTs are formed and combined together simultaneously. For example, CNTs containing magnetic iron oxide were obtained by chemical vapor deposition of coal gas with ferrocene as catalyst [20], by carbonization of iron-complex-doped polypyrrole nanotubes [21], and by a carbonization process using ferric chloride-embedded polyimide precursor [22].

(2) The second strategy is "inside-filling": iron oxide nanoparticles were encapsulated inside the hollow tubular structures of CNTs to produce magnetic nanotubes. There have been many studies on the fractionation of Fe_2O_3- or Fe_3O_4-filled carbon nanotubes [23–28].

(3) The third and more commonly used strategy is "outside-decorating": iron oxide nanoparticles were

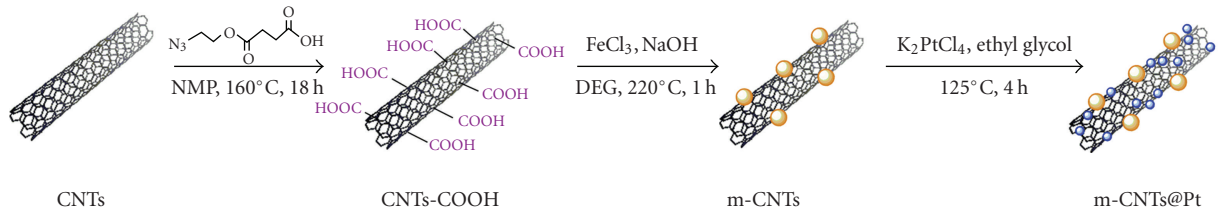

Scheme 1: Schematic description of the preparation of MWNTs-COOH, m-MWNTs, and m-MWNTs@Pt.

connected onto the outer convex surfaces of CNTs. This type of decorating can be generated, for instance, by in situ growth [17, 29], covalent [30], or noncovalent linkage [10] of functionalized magnetic nanoparticles.

On the other hand, CNTs are also suitable nanoparticle supports for heterogeneous catalysts due to their unique geometry and electronic properties [31]. The activities of CNTs-supported metal nanoparticles would be enhanced through metal-support interactions [32]. This phenomenon is presumably caused by the facts that CNTs are consisted of rolled graphene sheets with curved surface that changes the π-bonding in the graphene sheets, leading to different electronic structures. There have been plenty of reports about the decorating of CNTs with various noble metal nanoparticles such as Pt [33, 34], Pd [32], Ag [35, 36], and Au [37].

Recently, magnetic catalysts have received increasing attention because of the recycled use of the catalyst by an external magnetic field. However, the concept of magnetic catalyst made of magnetic CNTs and catalytic nanoparticles has never been presented and tried despite magnetic catalysts with other substrates such as silica spheres have been reported and demonstrated to be powerful in the reusable catalysts [38]. Based on their large surface area and the intrinsic electronic properties, CNTs would be a superior candidate for the magnetic catalyst support. But in the actual practice, there exist big challenges in the synthesis of CNT-supported magnetic catalysts, since (1) the loss of magnetism or noble nanoparticles is difficult to be avoided, and (2) it is difficult to load different nanoparticles independently on CNTs. So in the previous synthesis of magnetic nanocatalysts, the magnetic nanoparticles were usually stabilized by coating with a silica shell that could not only protect the magnetic particles from chemical attacking but also provide functional groups for subsequently loading the metal catalysts [38]. However, such a process would lead to complex experimental procedures and higher cost.

In this study, we present a facile and versatile approach to acquire CNT-supported magnetic catalysts. The synthesis method is simple and does not need any other stabilizing components. The carboxyl-functionalized CNTs were firstly decorated with Fe_3O_4 nanoparticles in a controlled manner and subsequently deposited with Pt nanoparticles by taking advantage of the unoccupied carboxyl groups on CNTs. The resulting Fe_3O_4/Pt nanoparticles decorated CNTs still maintain strong magnetism and catalytic activities. The superiorities of our approach are summarized as follows: (1) the superparamagnetic nanoparticles are highly crystalline, monodispersed, and evenly decorated on the convex surfaces of CNTs; (2) the fraction of magnetic nanoparticles deposited on CNTs and magnetic intensity of the resulting m-CNTs can be easily controlled to some extent by adjusting the feed ratio of the precursor to CNTs; (3) the synthesis process is simple, facile, and readily scalable, and the starting materials and other reagents are all commercially available, which will facilitate the large-scale and economically favorable production of m-CNTs catalysts; (4) this approach is in consonance with green chemistry principles. As the "green" concept has been highlighted by worldwide researchers nowadays, this approach is doomed to be promising with its environmentally harmonious features.

Moreover, we also studied the catalytic performance of the resulting catalysts in the reduction of 4-nitrophenol. Recycling the CNTs-supported catalytic nanoparticles can be easily accomplished by applying an external magnetic field, and the separated catalysts can be reused for many times. The novel Fe_3O_4/Pt nanoparticles decorated CNTs reported herein take advantage of both the unique properties of CNTs supports and the superparamagnetism of the Fe_3O_4 nanoparticles, offering promising applications in the heterogenerous catalysis.

2. Experimental

2.1. Materials. The pristine multriwalled carbon nanotubes (p-MWNTs) were purchased from Tsinghua-Nafine Nano-Powder Commercialization Engineering Center in Beijing (purity >95%). Anhydrous iron (III) chloride ($FeCl_3$, 98%) and diethylene glycol (DEG, 99%) were purchased from Alfa Aesar and used as received. Sodium hydroxide (NaOH, 99%) and ethanol were obtained from Sinopharm Chemical Reagent Co., Ltd. and used as received. The carboxyl-functionalized MWNTs (MWNTs-COOH) were prepared in our lab previously [33], and the density of carboxyl group was calculated to be 0.52 mmol (–COOH)/g from the corresponding TGA data.

2.2. Instrument. Thermal gravimetric analysis (TGA) was carried out on a TA Instruments TGA-2050 Thermogravimetric Analyzer with a heating rate of 20°C/min under a nitrogen flow rate of 60 mL/min. Transmission electron microscopy (TEM) and energy-dispersive X-ray spectrometer (EDS) analyses were performed on a JEOL JEM2010 electron microscope at 200 kV. X-ray diffraction (XRD)

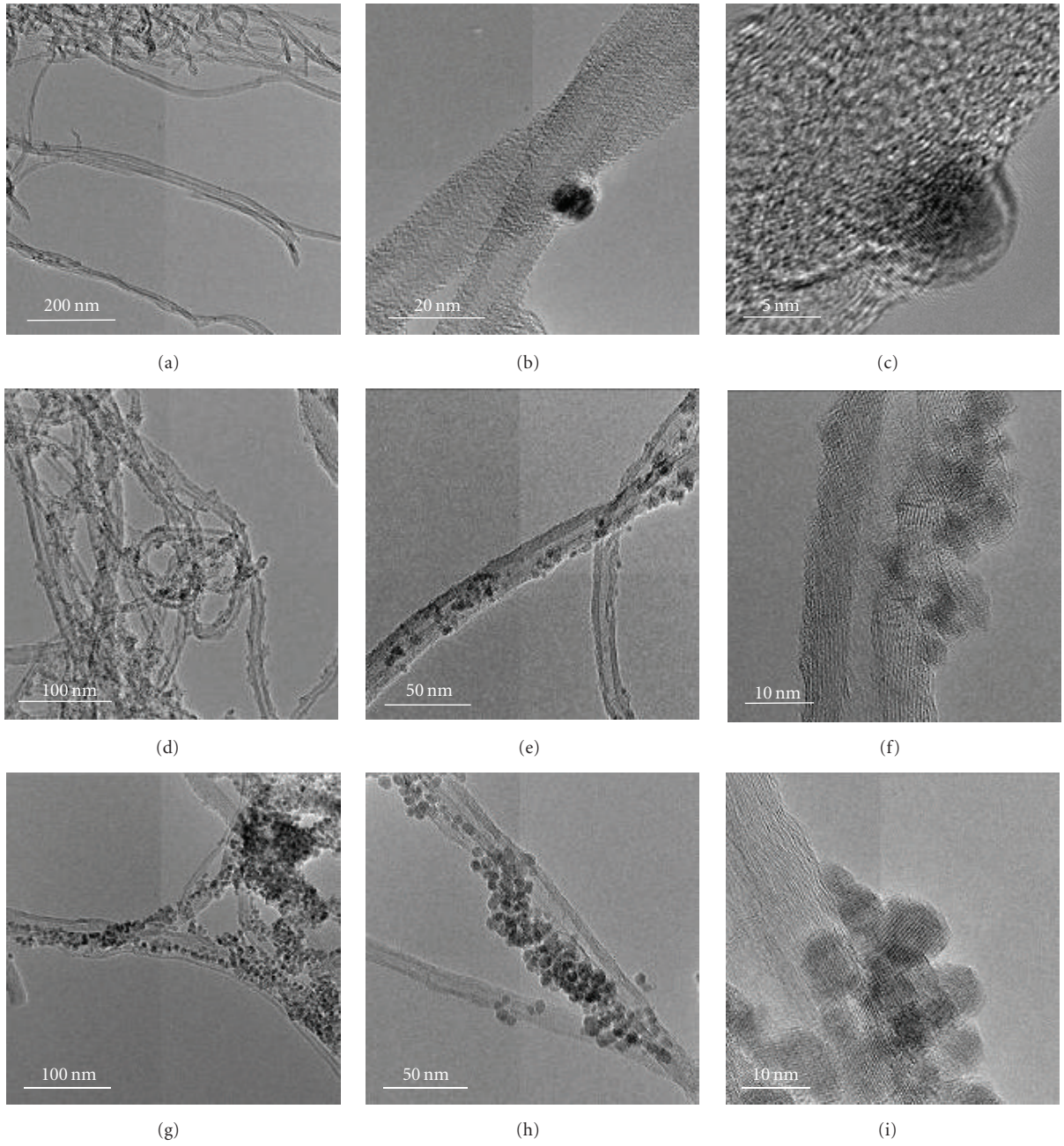

Figure 1: TEM images of p-MWNTs (a), m-MWNTs with feed ratios of 0.2/1 (b) and (c), 1/1 ((d)–(f)), and 5/1 ((g)–(i)).

patterns were recorded on a Rigaku X-ray diffractometer D/max-2200/PC equipped with Cu Kα radiation (40 kV, 20 mA) at the rate of 5.0 deg/min over the range of 10–70° (2θ). The magnetic properties were measured using a sample-vibrating magnetometer (VSM, Lake Shore 7410). Raman spectra were collected on a LabRam-1B Raman spectroscope equipped with a 632.8 nm laser source. UV-visible spectra were recorded using a Varian Cary 300 Bio UV—vis spectrophotometer.

2.3. Synthesis of Magnetic Multiwalled Carbon Nanotubes (m-MWNTs). First, a solution of NaOH dissolved in DEG (10 mg/mL) was prepared in advance. NaOH (100 mg, 2.5 mmol) was added into 10 mL of DEG under nitrogen and magnetic stirring, which was heated to 120°C for 1 hour, and then cooled down to 70°C and maintained for later use. In a typical synthesis of m-MWNTs (feed ratio = 1/1 (w/w)), MWNTs-COOH (30 mg) and DEG (10 mL) were placed in a three-neck round-bottom flask equipped with a condenser. The mixture was treated with an ultrasonic bath (40 kHz) for 1 minute and then placed on a magnetic stirrer with an oil bath. After $FeCl_3$ (63 mg, 0.388 mmol, the iron content was equivalent to 30 mg of Fe_3O_4) was added under nitrogen atmosphere and magnetic stirring, the mixture was

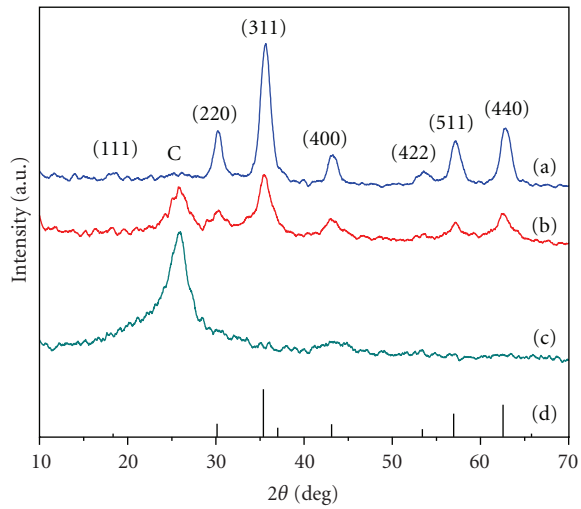

Figure 2: X-ray powder diffraction patterns for m-MWNTs with feed ratios of 5/1 (a), 1/1 (b), and 0.2/1 (c), and standard XRD peaks for magnetite (JCPDS card, file No. 19-0629).

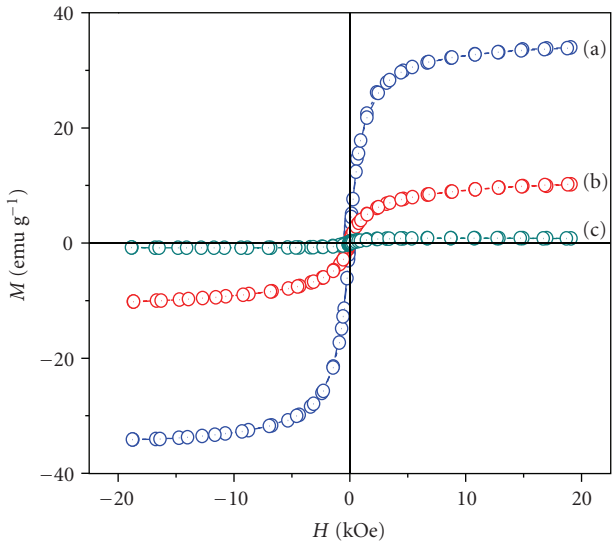

Figure 3: The curves of magnetic hysteresis loop at 300 K of m-MWNTs with feed ratios of 5/1 (a), 1/1 (b), and 0.2/1 (c).

then heated and maintained around 220°C for 30 minutes. A NaOH/DEG stock solution (5 mL) was injected quickly into the rapidly stirring mixture via a syringe. The resulting mixture was further heated at around 220°C for 1 hour. After cooling down to room temperature, the product was separated by centrifugation, redispersed in ethanol and collected by centrifugation several times, and then redispersed in water and collected by centrifugation several times. The black solid was dried under vacuum at 60°C overnight to give 48 mg of m-MWNTs. The same protocol was used to prepare m-MWNTs of different feed ratios, except that (1) for the synthesis of m-MWNTs (feed ratio = 1/5 (w/w)), $FeCl_3$ (0.325 g, 2 mmol) and NaOH/DEG solution (100 mg/mL, 2.5 mL) were used; and (2) for the synthesis of m-MWNTs ((feed ratio = 1/0.2 (w/w)), $FeCl_3$ (12.6 mg, 0.078 mmol) and NaOH/DEG solution (10 mg/mL, 1 mL) were used.

2.4. Synthesis of Pt Nanoparticles Decorated m-MWNTs (m-MWNTs@Pt). Typically, the as-prepared m-MWNTs (10 mg) and 10 mL of ethylene glycol-water solution (3 : 2 volume ratio) were placed into a 25 mL Schlenk flask, which was then treated with an ultrasonic bath (40 kHz) for 3 minute. K_2PtCl_4 (6.4 mg) was added into the reaction mixture and then heated in a 125°C oil bath under nitrogen atmosphere for 4 hour. The product was centrifuged, rinsed several times with deionized water, and dried under vacuum at 60°C.

3. Results and Discussion

3.1. Preparation and Characterization of m-MWNTs. The synthesis protocol of magnetic multiwalled carbon nanotubes (m-MWNTs) is illustrated in Scheme 1. Firstly, we used an improved one-step nitrene chemistry to functionalize CNTs [33]. The pristine multiwalled carbon nanotubes (p-MWNTs) were mixed with 4-(2-azidoethoxy)-4-oxobutanoic acid in N-methyl-2-pyrrolidinone (NMP), and the carboxyl groups were covalently linked on the surfaces of nanotubes by nitrene addition at elevated temperature, affording carboxyl-functionalized multiwalled carbon nanotubes (MWNTs-COOH). To produce m-MWNTs, we used a high-temperature solution-phase hydrolysis method [19, 39]. The Fe precursor, $FeCl_3$, was firstly coordinated to the carboxyl groups on the surfaces of MWNTs-COOH in diethylene glycol (DEG), then hydrolyzed upon the addition of NaOH at elevated temperature, and eventually dehydrated to in situ generate Fe_3O_4 nanoparticles.

It is worth noting that instead of using the most commonly used acid oxidation method, the MWNTs-COOH were prepared by the nitrene addition method, which has several advantages: (1) the pollutive acid (concentrated H_2SO_4/HNO_3) could be avoided, making the synthesis process cleaner and more convenient in practice; (2) the reaction is a weight increasing process and the reagents involved in the reaction are cheaply available in large quantity, making the synthesis economically favorable; (3) the severe erosion of CNTs by acid oxidation could be avoided, and thus the damages to the intrinsic morphology and properties of CNTs were significantly reduced. It is also worth mentioning that unlike some widely used iron sources including iron pentacarbonyl and iron acetylacetonate, the $FeCl_3$ (as well as the solvent DEG) used in the synthesis of m-CNTs is more environmentally friendly and inexpensive. Thus, the entire synthesis route (from the raw materials of CNTs to the final product of m-CNTs) is a totally clean, cheap, and green process.

In the synthesis of m-MWNTs, different feed ratios of $FeCl_3$ to MWNTs-COOH were used and the transmission electron microscopy (TEM) observation results are shown in Figure 1. The Fe_3O_4 nanoparticles appear as spherical nanocrystals that spread on the sidewalls of MWNTs. With the feed ratios raise from 0.2/1 to 1/1 and then to 5/1,

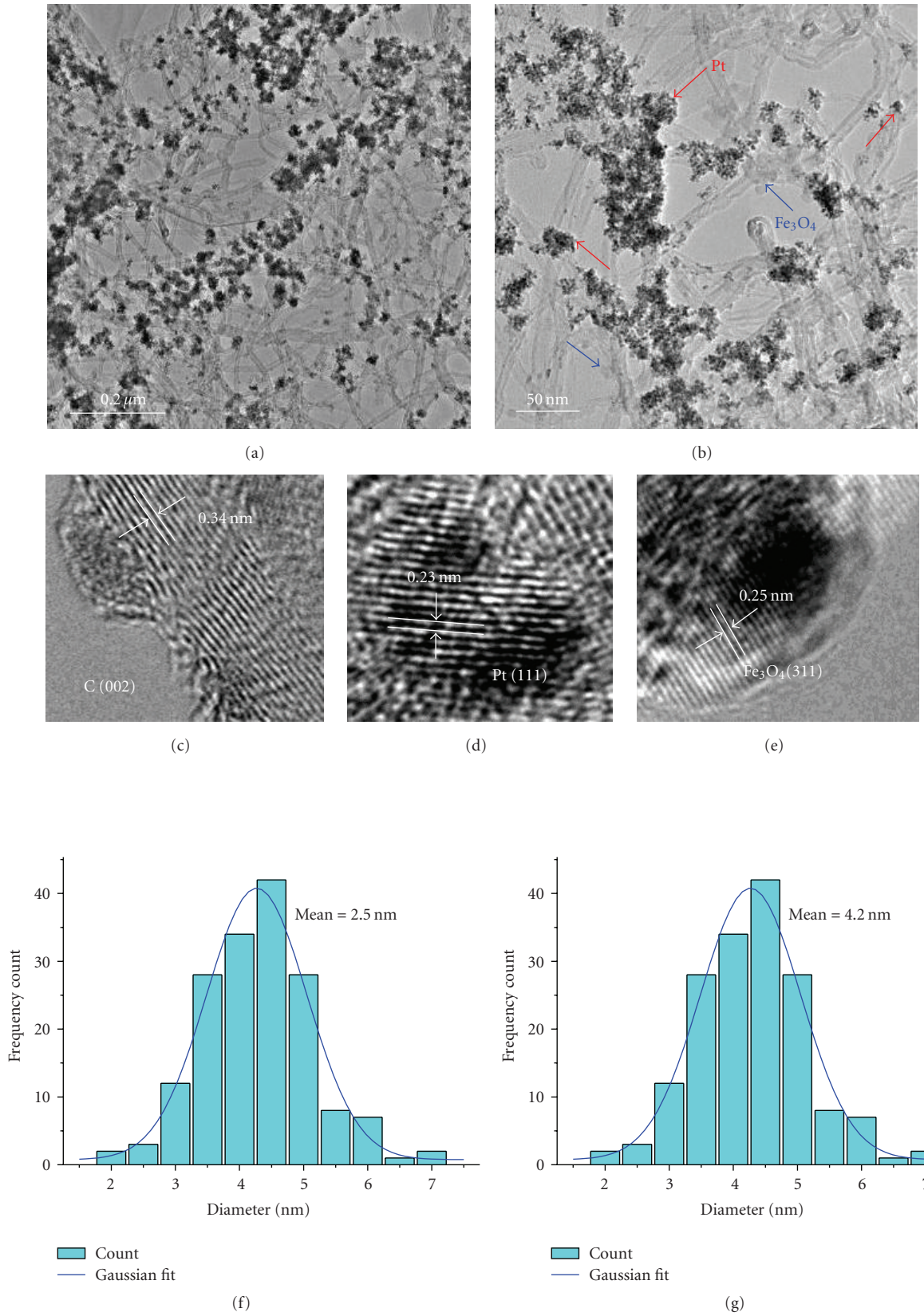

Figure 4: TEM images of m-MWNTs@Pt: low-resolution images ((a) and (b)), high-resolution images of the side walls of MWNTs (c), Pt nanoparticles (d), and Fe_3O_4 nanoparticles (e). The size distribution analysis of Pt nanoparticles (f) and Fe_3O_4 nanoparticles (g) of m-MWNTs@Pt.

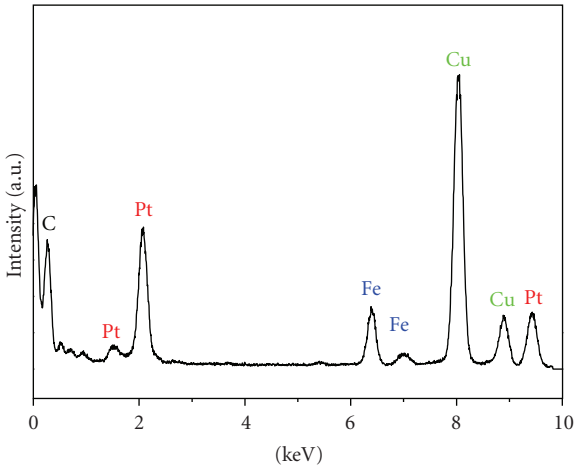

(a)

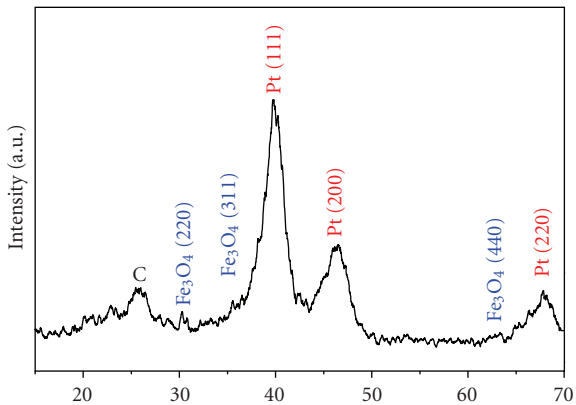

(b)

Figure 5: The EDS spectrum (a) and XRD pattern (b) of m-MWNTs@Pt.

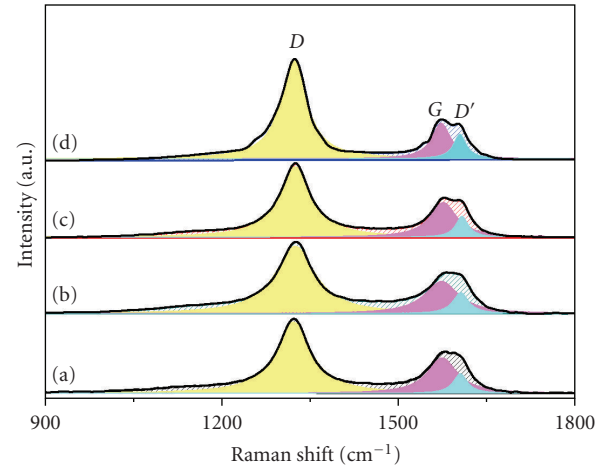

Figure 6: Raman spectra of p-MWNTs (a), MWNTs-COOH (b), m-MWNTs (c), and m-MWNTs@Pt (d).

the average sizes of Fe_3O_4 nanoparticles are all in the range of 4 ~ 5 nm, but the amounts of Fe_3O_4 nanoparticles on the nanotubes increase remarkably. It is concluded that there are plenty of carboxyl groups along the entire surfaces of MWNTs-COOH, and the relatively amounts of the carboxyl groups that are occupied and unoccupied by Fe_3O_4 nanoparticles can be adjusted by varying the feed ratios. The unoccupied carboxyl groups, thereby, could be used to deposit metal nanoparticles in the succeeding reaction.

In addition, the saturated magnetizations of m-MWNTs are also increased from 0.8 to 10.2 and then to 34.1 emu/g with the feed ratios raise from 0.2/1 to 1/1 and then to 5/1. As seen in Figure 2, the magnetic hysteresis loops of all these samples have no remanence or coercivity and exhibit superparamagnetic characteristics at room temperature. All of the resulting samples of m-MWNTs can move toward a magnet placed nearby, and the magnetic response is more obvious for the sample with higher feed ratio (see Figures S3, S5 and S7 in Supplementary Material available online at doi: 10.1155/2011/193510).

The X-ray diffraction (XRD) analysis in Figure 3 further proved that the nanoparticles on m-MWNTs have good crystalline quality and the diffraction peak positions fit well with the standard XRD data for magnetite (JCPDS card, file No. 19-0629). The diffraction peak at 2θ 25.9 is attributed to the graphite crystalline phase of CNTs, and the intensities of Fe_3O_4 diffraction peaks become stronger than those of CNTs with the enlarging of feed ratios.

In comparison, m-MWNTs could not be obtained in the control experiment using p-MWNTs instead of MWNTs-COOH as the templates, as confirmed by the TEM images in Figure S3. This is due to there are no carboxyl groups on p-MWNTs, and the Fe^{3+} ions could not be coordinated onto the surfaces of p-MWNTs to form Fe_3O_4 nanoparticles. Moreover, the oxidized MWNTs produced by a commonly used acid oxidation method [35] were also used in the control experiment and m-MWNTs could be successfully produced because of their abundant carboxyl groups (Figure S3).

3.2. Preparation and Characterization of m-MWNTs@Pt. Here we select Pt nanoparticles as a typical example of noble metal nanoparticles in this study to prepare Pt nanopartciles decorated m-MWNTs (m-MWNTs@Pt) by using K_2PtCl_4 as the Pt precursor and m-MWNTs as the templates via a solution-based method (Scheme 1). The m-MWNTs with feed ratio of 1/1 was chosen as the starting sample for the preparation of m-MWNTs@Pt since the decoration density of Fe_3O_4 nanoparticles is moderate and the magnetization is strong enough to enable them to be separated by magnetic force quickly. The residual carboxyl groups on the surfaces of m-MWNTs that are not occupied by Fe_3O_4 nanoparticles could serve as the nucleation centers for Pt nanoparticles. By mixing m-MWNTs and K_2PtCl_4 in ethylene glycol and heating at elevated temperature, the Pt nanoparticles were generated under the reductive atmosphere. Besides, by replacing $K_2PtCl_4$with different metal precursors and

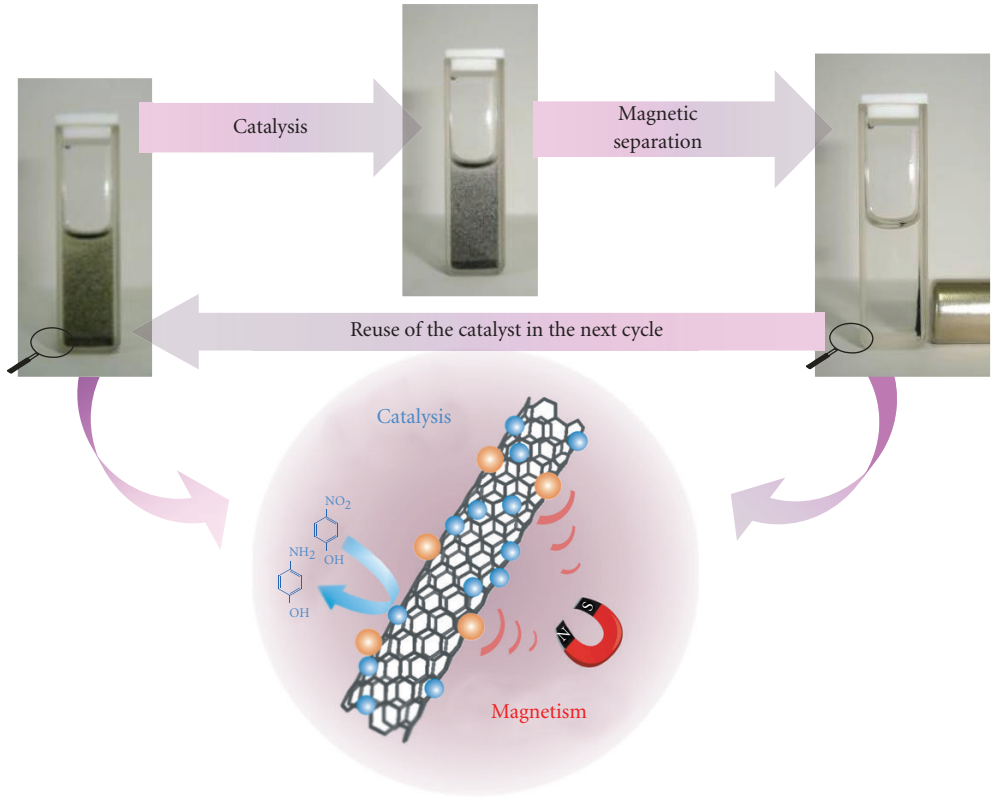

Scheme 2: The schematic illustration of the recycling of m-MWNTs@Pt for the catalytic reduction of 4-nitrophenol into 4-aminophenol in a quartz cuvette.

optimizing the synthesis conditions if necessary, we could probably obtain other kinds of metal nanoparticles (e.g., Pd, Au, Ag, Ru) decorated m-MWNTs.

The typical TEM images of m-MWNTs@Pt are shown in Figure 4. The Fe_3O_4 nanoparticles on MWNTs (marked by blue arrows) show the same scattered distribution pattern as those in Figures 1(d)–1(f), while the Pt nanoparticles mostly appear as nanoscale clusters that consist of many Pt nanoparticles (marked by red arrows). In the high-resolution TEM (HR-TEM) images of m-MWNTs@Pt (Figures 4(c)–4(e)), the lattice fringes of carbon walls (002), Pt(111), and Fe_3O_4 (311) were clearly observed, which denote that the sidewall structures of MWNTs were not spoiled after being modified with surface carboxyl groups and deposited with nanoparticles, and the Pt and Fe_3O_4 nanoparticles have good crystalline quality. The statistical sizes of Pt and Fe_3O_4 nanoparticles are 2.5 and 4.2 nm, respectively, with narrow size distributions (Figures 4(f) and 4(g)).

Figure 5(a) shows the EDS spectrum of m-MWNTs@Pt, revealing the presence of Fe and Pt elements on the carbon supports (the Cu signs origin from the TEM cupper grid loaded with the samples). From the EDS analysis results, it is also found that contents of Pt and Fe in m-MWNTs@Pt are 35.9 and 14.5 wt%, respectively. The crystalline structure of m-MWNTs@Pt was confirmed with powder XRD measurements (Figure 5(b)). The main reflection peaks of Fe_3O_4 and Pt crystals were clearly presented and the assignments of their peaks are indexed in Figure 5(b).

The Raman spectra for p-MWNTs, MWNTs-COOH, m-MWNTs, and m-MWNTs@Pt are shown in Figure 6. The G and D bands located around 1580 and 1320 cm^{-1} were clearly observed and are related to the vibration of sp^2-bonded carbon atoms in a 2D hexagonal lattice and the defects/disorder-induced modes, respectively [40]. The ratios of D- to G-band intensity (I_D/I_G) for MWNTs-COOH (2.44), m-MWNTs (2.48), and m-MWNTs@Pt (3.81) are greater than those of p-MWNTs (2.38), which are resulted from the increase in the degree of disorder after functionalization of MWNTs. The D'-bands around 1602 cm^{-1} are not very distinct for the p-MWNTs and MWNTs-COOH, but they become more obvious for m-MWNTs and m-MWNTs@Pt, indicating the defects and disorder of MWNTs increase after functionalization [41].

3.3. Catalysis Applications. The catalysis activity of the resulting sample of m-MWNTs@Pt is measured by using a model reaction of the catalytic reduction of 4-nitrophenol into 4-aminophenol with $NaBH_4$, which has been demonstrated to be an effective way to evaluate the catalytic capability of noble metal nanocatalysts [38, 42–44]. The ultraviolet-visible (UV-vis) spectroscopy was used to monitor the reduction process, and the results for the first reduction

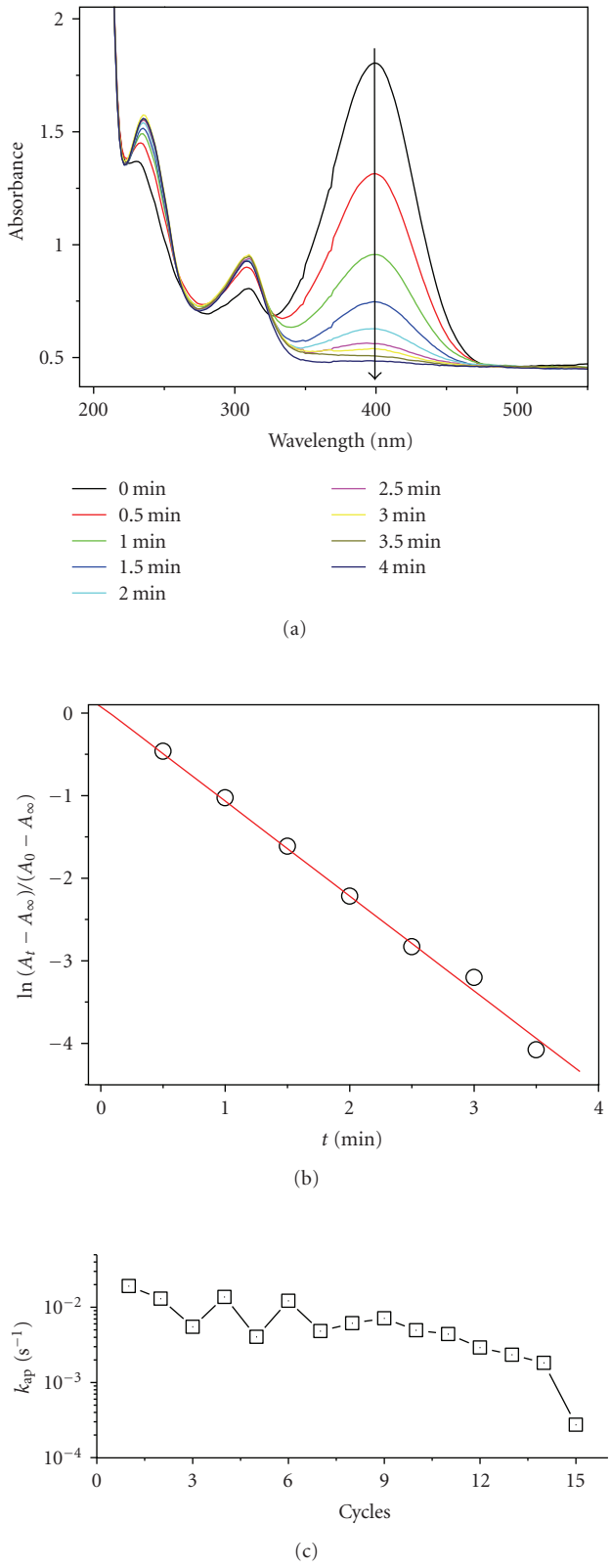

Figure 7: (a) Successive UV-vis spectra for the reduction of 4-nitrophenol into 4-aminophenol with the catalyst of m-MWNTs@Pt in the first cycle. (b) The linearized data for first-order analysis corresponding to (a). (c) The calculated values of kobs in the fifteen successive cycles of reduction and magnetic separation with the catalyst of m-MWNTs@Pt.

cycle are shown in Figure 7(a). Before the catalysts were added, the characteristic absorption peak of 4-nitrophenol located at 400 nm remained constant, suggesting no reduction is occurred. Once the catalysts were added into the reaction mixture, the peak at 400 nm decreased quickly and completely disappeared within several minutes. Meanwhile, a new peak at 290 nm appeared that was attributed to 4-aminophenol. The reduction could also be clearly observed by naked eyes since the yellow color of 4-nitrophenol solution gradually faded out during the reduction process (Scheme 2).

The concentration of $NaBH_4$ greatly exceeded those of 4-nitrophenol and the catalyst and remained essentially constant during the reduction. Therefore, the kinetics of this reduction is supposed to follow pseudo-first-order to the concentration of 4-nitrophenol, and the kinetic equation can be defined as follows:

$$\ln\left(\frac{A_t - A_\infty}{A_0 - A_\infty}\right) = -k_{ap}t, \quad (1)$$

where t is the reaction time, A_0 is the initial absorbance at time zero, A_t is the absorbance at time t, A_∞ is the absorbance when the reaction is completed, and k_{ap} is the apparent rate constant [45]. As seen in Figure 7(b), the linear-fit plot coincides with (1), indicating the pseudo-first-order kinetics of this reduction with m-MWNTs@Pt. When the reduction is completed, the m-MWNTs@Pt could be quickly separated from the reaction system by applying an external magnetic field. The magnetically separated m-MWNTs@Pt could be reused in the next run of the same catalytic reaction. It is found that the m-MWNTs@Pt still possess catalytic activity even after 15 consecutive cycles of catalytic reduction and magnetic separation. In each cycle of catalytic reduction, the data show good linear correlation with time as (1) (Figure S7). The calculated values of k_{ap} in the fifteen successive cycles of catalytic reduction are shown in Figure 7(c). The values of k_{ap} exhibit a general trend of decrease with the increase of the number of cycles (from $1.92 \times 10^{-2}\,s^{-1}$ for cycle 1 to $2.74 \times 10^{-4}\,s^{-1}$ for cycle 15). The changing range of k_{ap} is comparable with or higher than some other types of supported metal nanocatalysts, such as dendrimer-metal nanocomposites ($10^{-5} \sim 10^{-1}\,s^{-1}$) [42, 46] and SiO_2-Pt nanohybrids ($\sim 10^{-3}\,s^{-1}$) [38]. The large values of k_{ap} in the successive cycles of catalytic reduction (even after 15 cycles) demonstrated the high catalytic activity of m-MWNTs@Pt and the feasibility to use them as magnetically recyclable catalysts.

4. Conclusions

In summary, we developed a novel kind of Fe_3O_4/Pt nanoparticles decorated CNTs for use as the magnetically recyclable catalysts for the first time. The synthesis of magnetic CNTs is facile, well controllable, and readily scalable. The resulting catalysts show high catalytic activity in the reduction of 4-nitrophenol and can be reused for at least fifteen cycles. The superparamagnetic property of the catalysts enables them to be easily separated by an external

magnetic field, which greatly facilities the recycle of the catalysts. This synthesis approach reported here is a general one that is expected to be applicable with (1) different types of CNTs: single-walled, double-walled, and multiwalled carbon nanotubes; (2) different types of magnetic nanoparticles: Fe_3O_4, γ-Fe_2O_3, Co, CoO, Ni, and so forth; (3) different embedding types of magnetic nanoparticles to the CNTs: inside-filling, outside-decorating, and so forth; (4) different types of metals: Pt, Pd, Ag, Au, Ru, and so forth; and (5) different types of catalytic reactions: hydrogenation, oxidation of alcohols, Heck reaction, and so forth. It is believed that the novel CNTs-supported magnetically recyclable catalysts will find important applications in heterogeneous catalysis.

Acknowledgments

This work was financially supported by the National Natural Science Foundation of China (nos. 50773038 and 20974093), National Basic Research Program of China (973 Program) (no. 2007CB936000), the Fundamental Research Funds for the Central Universities (2009QNA4040), Qianjiang Talent Foundation of Zhejiang Province (2010R10021), and the Foundation for the Author of National Excellent Doctoral Dissertation of China (no. 200527).

References

[1] S. Iijima, "Helical microtubules of graphitic carbon," *Nature*, vol. 354, no. 6348, pp. 56–58, 1991.

[2] L. Dai and A. W. H. Mau, "Controlled synthesis and modification of carbon nanotubes and C_{60}: carbon nanostructures for advanced polymeric composite materials," *Advanced Materials*, vol. 13, no. 12-13, pp. 899–913, 2001.

[3] S. Niyogi, M. A. Hamon, H. Hu et al., "Chemistry of single-walled carbon nanotubes," *Accounts of Chemical Research*, vol. 35, no. 12, pp. 1105–1113, 2002.

[4] H. Dai, "Carbon nanotubes: synthesis, integration, and properties," *Accounts of Chemical Research*, vol. 35, no. 12, pp. 1035–1044, 2002.

[5] R. H. Baughman, A. A. Zakhidov, and W. A. De Heer, "Carbon nanotubes—the route toward applications," *Science*, vol. 297, no. 5582, pp. 787–792, 2002.

[6] V. Georgakilas, D. Gournis, V. Tzitzios, L. Pasquato, D. M. Guldi, and M. Prato, "Decorating carbon nanotubes with metal or semiconductor nanoparticles," *Journal of Materials Chemistry*, vol. 17, no. 26, pp. 2679–2694, 2007.

[7] D. Eder, "Carbon nanotube-inorganic hybrids," *Chemical Reviews*, vol. 110, no. 3, pp. 1348–1385, 2010.

[8] C. Gao, W. Li, H. Morimoto, Y. Nagaoka, and T. Maekawa, "Magnetic carbon nanotubes: synthesis by electrostatic self-assembly approach and application in biomanipulations," *Journal of Physical Chemistry B*, vol. 110, no. 14, pp. 7213–7220, 2006.

[9] W. Li, C. Gao, H. Qian, J. Ren, and D. Yan, "Multiamino-functionalized carbon nanotubes and their applications in loading quantum dots and magnetic nanoparticles," *Journal of Materials Chemistry*, vol. 16, no. 19, pp. 1852–1859, 2006.

[10] M. A. Correa-Duarte, M. Grzelczak, V. Salgueiriño-Maceira et al., "Alignment of carbon nanotubes under low magnetic fields through attachment of magnetic nanoparticles," *Journal of Physical Chemistry B*, vol. 109, no. 41, pp. 19060–19063, 2005.

[11] C. Richard, B.-T. Doan, J.-C. Beloeil, M. Bessodes, É. Tóth, and D. Scherman, "Noncovalent functionalization of carbon nanotubes with amphiphilic Cd^{3+} chelates: toward powerful T_1 and T_2 MRI contrast agents," *Nano Letters*, vol. 8, no. 1, pp. 232–236, 2008.

[12] Z. Liu, S. Tabakman, K. Welsher, and H. Dai, "Carbon nanotubes in biology and medicine: in vitro and in vivo detection, imaging and drug delivery," *Nano Research*, vol. 2, no. 2, pp. 85–120, 2009.

[13] D. Gozzi, A. Latini, G. Capannelli et al., "Synthesis and magnetic characterization of Ni nanoparticles and Ni nanoparticles in multiwalled carbon nanotubes," *Journal of Alloys and Compounds*, vol. 419, no. 1-2, pp. 32–39, 2006.

[14] R. Kozhuharova, M. Ritschel, D. Elefant et al., "Well-aligned Co-filled carbon nanotubes: preparation and magnetic properties," *Applied Surface Science*, vol. 238, no. 1–4, pp. 355–359, 2004.

[15] H. Zhang, N. Du, P. Wu, B. Chen, and D. Yang, "Functionalization of carbon nanotubes with magnetic nanoparticles: general nonaqueous synthesis and magnetic properties," *Nanotechnology*, vol. 19, no. 31, Article ID 315604, 2008.

[16] Y. Li, T. Kaneko, T. Ogawa, M. Takahashi, and R. Hatakeyama, "Magnetic characterization of Fe-nanoparticles encapsulated single-walled carbon nanotubes," *Chemical Communications*, no. 3, pp. 254–256, 2007.

[17] J. Wan, W. Cai, J. Feng, X. Meng, and E. Liu, "*In situ* decoration of carbon nanotubes with nearly monodisperse magnetite nanoparticles in liquid polyols," *Journal of Materials Chemistry*, vol. 17, no. 12, pp. 1188–1192, 2007.

[18] I. Brigger, C. Dubernet, and P. Couvreur, "Nanoparticles in cancer therapy and diagnosis," *Advanced Drug Delivery Reviews*, vol. 54, no. 5, pp. 631–651, 2002.

[19] J. Ge, Y. Hu, M. Biasini, W. P. Beyermann, and Y. Yin, "Superparamagnetic magnetite colloidal nanocrystal clusters," *Angewandte Chemie International Edition*, vol. 46, no. 23, pp. 4342–4345, 2007.

[20] J. Qiu, Q. Li, Z. Wang, Y. Sun, and H. Zhang, "CVD synthesis of coal-gas-derived carbon nanotubes and nanocapsules containing magnetic iron carbide and oxide," *Carbon*, vol. 44, no. 12, pp. 2565–2568, 2006.

[21] J. Jang and H. Yoon, "Fabrication of magnetic carbon nanotubes using a metal-impregnated polymer precursor," *Advanced Materials*, vol. 15, no. 24, pp. 2088–2091, 2003.

[22] J. Jang, K. J. Lee, and Y. Kim, "Fabrication of polyimide nanotubes and carbon nanotubes containing magnetic iron oxide in confinement," *Chemical Communications*, no. 30, pp. 3847–3849, 2005.

[23] G. Korneva, H. Ye, Y. Gogotsi et al., "Carbon nanotubes loaded with magnetic particles," *Nano Letters*, vol. 5, no. 5, pp. 879–884, 2005.

[24] W. Chen, X. Pan, M.-G. Willinger, D. S. Su, and X. Bao, "Facile autoreduction of iron oxide/carbon nanotube encapsulates," *Journal of the American Chemical Society*, vol. 128, no. 10, pp. 3136–3137, 2006.

[25] W. Chen, X. Pan, and X. Bao, "Tuning of redox properties of iron and iron oxides via encapsulation within carbon nanotubes," *Journal of the American Chemical Society*, vol. 129, no. 23, pp. 7421–7426, 2007.

[26] F. Cao, K. Zhong, A. Gao, C. Chen, Q. Li, and Q. Chen, "Reducing reaction of Fe_3O_4 in nanoscopic reactors of a-CNTs," *Journal of Physical Chemistry B*, vol. 111, no. 7, pp. 1724–1728, 2007.

[27] S. Qu, F. Huang, G. Chen, S. Yu, and J. Kong, "Magnetic assembled electrochemical platform using Fe_2O_3 filled carbon nanotubes and enzyme," *Electrochemistry Communications*, vol. 9, no. 12, pp. 2812–2816, 2007.

[28] B. T. Hang, H. Hayashi, S.-H. Yoon, S. Okada, and J.-I. Yamaki, "Fe_2O_3-filled carbon nanotubes as a negative electrode for an Fe-air battery," *Journal of Power Sources*, vol. 178, no. 1, pp. 393–401, 2008.

[29] S. F. Chin, K. S. Iyer, and C. L. Raston, "Fabrication of carbon nano-tubes decorated with ultra fine superparamagnetic nano-particles under continuous flow conditions," *Lab on a Chip*, vol. 8, no. 3, pp. 439–442, 2008.

[30] H. He, Y. Zhang, C. Gao, and J. Wu, "'Clicked' magnetic nanohybrids with a soft polymer interlayer," *Chemical Communications*, no. 13, pp. 1655–1657, 2009.

[31] G. G. Wildgoose, C. E. Banks, and R. G. Compton, "Metal nanoparticles and related materials supported on Carbon nanotubes: methods and applications," *Small*, vol. 2, no. 2, pp. 182–193, 2006.

[32] Y. S. Chun, J. Y. Shin, C. E. Song, and S.-G. Lee, "Palladium nanoparticles supported onto ionic carbon nanotubes as robust recyclable catalysts in an ionic liquid," *Chemical Communications*, no. 8, pp. 942–944, 2008.

[33] C. Gao, H. He, L. Zhou, X. Zheng, and Y. Zhang, "Scalable functional group engineering of carbon nanotubes by improved one-step nitrene chemistry," *Chemistry of Materials*, vol. 21, no. 2, pp. 360–370, 2009.

[34] A. Kaniyoor, R. I. Jafri, T. Arockiadoss, and S. Ramaprabhu, "Nanostructured Pt decorated graphene and multi walled carbon nanotube based room temperature hydrogen gas sensor," *Nanoscale*, vol. 1, no. 3, pp. 382–386, 2009.

[35] C. Gao, C. D. Vo, Y. Z. Jin, W. Li, and S. P. Armes, "Multihydroxy polymer-functionalized carbon nanotubes: synthesis, derivatization, and metal loading," *Macromolecules*, vol. 38, no. 21, pp. 8634–8648, 2005.

[36] C. Gao, W. Li, Y. Z. Jin, and H. Kong, "Facile and large-scale synthesis and characterization of carbon nanotube/silver nanocrystal nanohybrids," *Nanotechnology*, vol. 17, no. 12, article 010, pp. 2882–2890, 2006.

[37] H. C. Choi, M. Shim, S. Bangsaruntip, and H. Dai, "Spontaneous reduction of metal ions on the sidewalls of carbon nanotubes," *Journal of the American Chemical Society*, vol. 124, no. 31, pp. 9058–9059, 2002.

[38] L. Zhou, C. Gao, and W. Xu, "Robust Fe_3O_4/SiO_2-Pt/Au/Pd magnetic nanocatalysts with multifunctional hyperbranched polyglycerol amplifiers," *Langmuir*, vol. 26, no. 13, pp. 11217–11225, 2010.

[39] J. Ge, Y. Hu, M. Biasini et al., "One-step synthesis of highly water-soluble magnetite colloidal nanocrystals," *Chemistry*, vol. 13, no. 25, pp. 7153–7161, 2007.

[40] Y. Zhang, H. K. He, and G. Chao, "Clickable macroinitiator strategy to build amphiphilic polymer brushes on carbon nanotubes," *Macromolecules*, vol. 41, no. 24, pp. 9581–9594, 2008.

[41] Y. Zhang, H. He, C. Gao, and J. Wu, "Covalent layer-by-layer functionalization of multiwalled carbon nanotubes by click chemistry," *Langmuir*, vol. 25, no. 10, pp. 5814–5824, 2009.

[42] K. Esumi, R. Isono, and T. Yoshimura, "Preparation of PAMAM- and PPI-Metal (Slver, Platinum, and Palladium) nanocomposites and their catalytic activities for reduction of 4-nitrophenol," *Langmuir*, vol. 20, no. 1, pp. 237–243, 2004.

[43] J. Wu, H. He, and C. Gao, "β-Cyclodextrin-capped polyrotaxanes: one-pot facile synthesis via click chemistry and use as templates for platinum nanowires," *Macromolecules*, vol. 43, no. 5, pp. 2252–2260, 2010.

[44] H. He and C. Gao, "A general strategy for the preparation of carbon nanotubes and graphene oxide decorated with PdO nanoparticles in water," *Molecules*, vol. 15, no. 7, pp. 4679–4694, 2010.

[45] I. Pastoriza-Santos, J. Pérez-Juste, S. Carregal-Romero, P. Hervés, and L. M. Liz-Marzán, "Metallodielectric hollow shells: optical and catalytic properties," *Chemistry*, vol. 1, no. 5, pp. 730–736, 2006.

[46] K. Esumi, K. Miyamoto, and T. Yoshimura, "Comparison of PAMAM-Au and PPI-Au nanocomposites and their catalytic activity for reduction of 4-nitrophenol," *Journal of Colloid and Interface Science*, vol. 254, no. 2, pp. 402–405, 2002.